Cambridge Centre for Computational Chemical Engineering

University of Cambridge

Department of Chemical Engineering

Preprint ISSN 1473 – 4273

Modelling Soot Formation in a DISI Engine

Jonathan Etheridge [1] Sebastian Mosbach [1] Markus Kraft [1] Hao Wu [2]

Nick Collings [2]

released: 11 January 2010

[1] Department of Chemical Engineering
University of Cambridge
New Museums Site
Pembroke Street
Cambridge, CB2 3RA
UK
E-mail: mk306@cam.ac.uk

[2] Department of Engineering
University of Cambridge
Trumpington Street
Cambridge, CB2 1PZ
UK

Preprint No. 90

c4e

Key words and phrases: DISI engine modelling, detailed chemistry, soot

Edited by
Cambridge Centre for Computational Chemical Engineering
Department of Chemical Engineering
University of Cambridge
Cambridge CB2 3RA
United Kingdom.

Fax: + 44 (0)1223 334796
E-Mail: c4e@cheng.cam.ac.uk
World Wide Web: http://www.cheng.cam.ac.uk/c4e/

Abstract

In this work, the formation of soot in a Direct Injection Spark Ignition (DISI) engine is simulated using the Stochastic Reactor Model (SRM) engine code. Volume change, convective heat transfer, turbulent mixing, direct injection and flame propagation are accounted for. In order to simulate flame propagation, the cylinder is divided into an unburned, entrained and burned zone, with the rate of entrainment being governed by empirical equations but combustion modeled with chemical kinetics. The model contains a detailed chemical mechanism as well as a highly detailed soot formation model, however computation times are relatively short. The soot model provides information on the morphology and chemical composition of soot aggregates along with bulk quantities, including soot mass, number density, volume fraction and surface area. The model is first calibrated by simulating experimental data from a Gasoline Direct Injection (GDI) Spark Ignition (SI) engine. The model is then used to simulate experimental data from the literature, where the numbers, sizes and derived mass particulate emissions from a 1.83 L, 4-cylinder, 4 valve production DISI engine were examined. Experimental results from different injection and spark timings are compared with the model and the qualitative trends in aggregate size distribution and emissions match the exhaust gas measurements well.

Contents

1 Introduction **3**

2 Model Details **3**

2.1 Engine Model 4

2.2 Soot Model 6

3 Model Calibration **7**

4 Results **9**

5 Conclusions **11**

1 Introduction

Direct injection stratified charge (DISC) Spark Ignition (SI) engines can offer up to 25% improvement in fuel economy compared with port-fuel injected (PFI) SI engines [1]. This is mainly achieved through reductions in pumping and heat losses when operated unthrottled at low-mid loads. One of the drawbacks however is the increase in particulate emissions formed by combustion of fuel rich regions in the cylinder [2].

Several different methods for modelling Direct Injection Spark Ignition (DISI) engines have been employed. The in-cylinder fuel stratification makes simulation more taxing compared with port fueled SI engines or GDI SI engines with early fuel injection, where the in-cylinder charge can be assumed homogenous. The Coherent Flame Model has been extended to stratified combustion [3]. An assumed Probability Density Function (PDF) approach has been used with Computational Fluid Dynamics (CFD) to model experimental DISI engine data [4]. Another CFD attempt used a modified version of the BML flamelet approach [5]. More recently a Spark Channel Ignition Monitoring Model (SparkCIMM) was successfully developed and used to model the small scale spark formation [6]. The G-equation flamelet combustion model was used to track the flame front when the surface was large enough. Both models take into account local mixture fraction variance. CFD models are an important tool for investigating in-cylinder mixing and the effects of spray and cylinder geometry in DISI combustion.

However, incorporating detailed chemical kinetics into these models remains computationally expensive and investigation of DISI engine soot has not been attempted. Engine soot modelling in the literature has been mainly aimed at diesel engines and mostly uses empirical soot models [7, 8]. Models based on the method of moments have also been used [9]. The CFD code KIVA is commonly used as a base for such engine simulations. Recent soot models have increased in detail [10], however they only use a small number of quantities and neglect the chemical composition of the soot particles which strongly affects reaction rates.

The aim of this paper is to present an engine model which can be used to simulate soot formation in a DISI engine. The model incorporates a very detailed soot model. To the authors' knowledge this is the first attempt at detailed soot modelling in an SI engine. The model is first validated by simulating a GDI engine with early injection. The model is then used to simulate soot formation in a DISI engine operated with a stratified charge.

The paper is structured as follows. Firstly the engine and soot model details are explained. In the following section, results from the model, calibrated using experimental data from a GDI SI engine operated with an early injection to produce a largely premixed charge, are presented. The model is then used to simulate a stratified charge SI engine and the emissions are compared with experimental results from the literature.

2 Model Details

In this section the engine model and integrated soot model are briefly described. The model was previously used to simulate soot in an HCCI engine and further details on the

integrated engine and soot model can be found in [11].The focus in this work is to address at least some of the challenges of soot modelling associated to DISI engines.

2.1 Engine Model

The Stochastic Reactor Model (SRM) is a spatially zero dimensional model based on Probability Density Function (PDF) transport methods [12]. The cylinder charge is split into an ensemble of particles that represent the distribution of temperature, pressure and concentration of chemical species within the engine cylinder. The method allows detailed chemistry calculations with relatively short computational times. Details of the chemical mechanism, containing 208 species and 1002 reactions, are provided in [11]. In-cylinder turbulent mixing is accounted for using the Euclidean Minimum Spanning Tree (EMST) mixing model [13]. Stochastic heat transfer, piston movement and direct injection sub-models are also included [14]. The model has been successfully employed for HCCI simulation [14–17]. A flame propagation model has been added to enable SI simulation and full details are given in [18].

For SI simulation the particle ensemble is divided into three zones: unburned, entrained and burned. Mixing occurs within each zone but not between zones and all particles are initially in the unburned zone. Mass transfer between zones is described below. The Euclidean Minimum Spanning Tree (EMST) mixing model is used in the unburned and burned zones and is described in [13]. The entrained zone is subdivided into unburned and burning particle categories to keep track of the particles' states. Chemistry occurs at every CAD step in every particle as in the HCCI model.

The diameter of the entrained zone at the time of spark was set to 1.0 mm, the rough size of the spark gap. The first particle randomly chosen to enter the entrained zone is not added all at once but the actual entrained volume is removed from it and added to a new particle in the entrained zone. Once the entrained volume has increased above the particle's volume, it is reunited into a single particle. The spark is simulated by setting the temperature of the mass added to the entrained zone at each step to 2000 K, until all of the spark energy has been added.

A particle is moved from the unburned zone to the entrained zone when the calculated flame volume exceeds the burned and entrained zone volumes by more than half the volume of the next particle to be entrained. For DISI simulation a particle is chosen with a probability proportional to the concentration of fuel in the particle. The volume of the flame is calculated from the geometry of the piston and cylinder, and the flame radius assuming it is spherical and centred at the spark location. The flame radius at the n^{th} time step, $R_{f;n}$, is obtained from

$$R_{f;n} = R_{f;n-1} + \left(u_T \left(1 - \exp\left(\frac{-(t - t_{spark})}{\tau_b} \right) \right) + S_L \right) \Delta t. \tag{1}$$

The increase in flame radius is calculated as the time step multiplied by the entrainment velocity. The radius initially increases at the laminar flame speed, S_L,until a wrinkled turbulent flame front develops after a characteristic burn time, τ_b [19, 20]. The characteristic

burn time is given by

$$\tau_b = \frac{l_T}{S_L}, \tag{2}$$

where l_T is the characteristic length scale [20].

The mixing time in the entrained zone, τ_E, is increased at the same exponential rate as the transition from a laminar to a turbulent flame. The mixing time increases to the value τ_E^{max} once the turbulent flame has fully developed. Before this the entrained zone mixing time is smaller causing faster mixing and heat release. This was included as the rate of burning is initially the rate of entrainment before a turbulent flame front has developed containing unburned pockets [21].

$$\tau_E = \tau_E^{max}\left(1 - \exp\left(\frac{-(t - t_{spark})}{\tau_b}\right)\right) \tag{3}$$

The rate of burning is controlled by the mass entrained and the rate it mixes with the hot, reacting entrained material and is calculated with the detailed chemical mechanism. The correlation used to obtain the characteristic flame speed, u_T, was taken from [22]:

$$u_T = 0.08C\bar{u}_i\left(\frac{\rho_u}{\rho_i}\right)^{1/2}, \tag{4}$$

where $\bar{u}_i$ is the mean inlet gas speed, ρ_u is the unburned gas density and ρ_i is the inlet air density.

The cylinder geometry model contains a pent roof and the piston contains a bowl. The volume of the spherical flame is calculated exactly in the bowl and cylinder areas. In the pent roof region numerical integration of the flame cross sectional area at different heights is used to obtain the flame volume.

Particles are moved from the entrained and unburned zone to the entrained and burning zone when their temperature has risen above 1500 K. During the chemistry step the rate of heat release in each entrained particle is calculated. When the heat release rate of an entrained particle has dropped below 2 % of its maximum heat release rate, the particle is moved to the burned zone. Particles are also transferred from the entrained zone to the burned zone if they remain in the entrained zone for the maximum length of time, t_E^{max}. This was included in the model to prevent particles that do not combust from remaining in the entrained zone throughout the simulation. When no particles remain in the unburned zone, the entrained zone mixing time is set to τ_E^{max} as equation (2) can no longer be evaluated.

One of the most desirable features of the EMST mixing model is that it preferentially mixes particles which are close in composition space. This is based on the reasoning that fluid parcels which are close in physical space should be similar in terms of composition. The EMST mixing model was previously used in the entrained zone to simulate combustion in a conventional SI engine. This however caused mixing in the entrained zone to mostly occur between freshly entrained particles and between the burning entrained particles. The entrained particles were then nearly homogeneous before mixing with the burning particles and igniting. The flame brush is relatively thin with high temperature

and concentration gradients across it so EMST is not a good mixing model to use in the entrained zone for the low number of particles used in the simulation.

Therefore we decided to use Curl's mixing model in the entrained zone [23], whereby two particles are selected to mix. The difference being that only unburned entrained particles are chosen to mix with entrained and burning particles. The resulting particle compositions are not identical as the particles only move to their mean composition by a factor of 10 % and the mixing time is accordingly adjusted to reflect this. This method was chosen to prevent the entrained zone from becoming unphysically homogeneous.

2.2 Soot Model

A detailed set of population balance equations is used to model soot formation. The solver is based on a Monte Carlo method [24, 25] and is implemented in a library called SWEEP [26].

The surface area, S_a, the number of primary particles, N_PP and primary particle j diameters, d_j^PP (assuming sphericity) are tracked for each aggregate. The number of of carbon atoms, C, the number of hydrogen atoms, H, and the number of PAH molecules ,N_PAH, are also stored and make up the individual aggregate's chemical composition. The number of functional sites are tracked using the Aromatic Site Counting Model [27]. The site types considered here are free edge, armchair, zigzag, and bay sites, and five-membered rings (Fig. 1), with numbers N_ed, N_ac, N_zz, N_bay, and N_R5 respectively.

The statistical representation of PAHs and their functional sites provides a detailed soot aggregate description but remains computationally efficient compared with tracking every single molecule. The number of internal co-ordinates is large which is why Monte Carlo methods are employed.

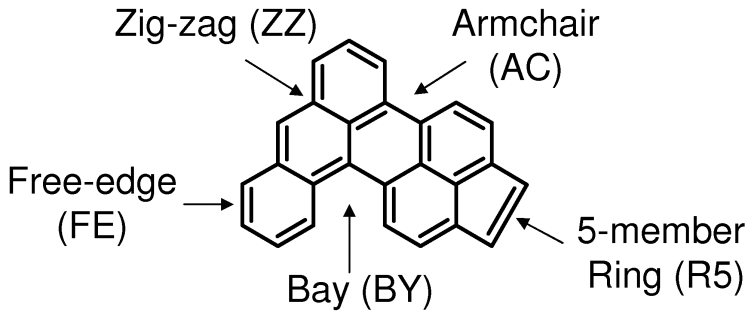

Figure 1: *Types of functional sites on the edge of a PAH molecule.*

The pathways included in the model that enable mass transfer from the gas phase to the particulate phase are inception, condensation and surface growth. Coagulation and surface growth are modelled in the particulate phase. The surface chemistry includes growth and oxidation reactions [28]. The rates of the surface reactions depend on the attacked functional site and also the neighboring ones. This information can be provided through statistical correlations obtained from Kinetic Monte Carlo (KMC) simulations [28]. For the computational speed-up of surface reactions the Linear Process Deferment Algorithm (LPDA) [29] is employed.

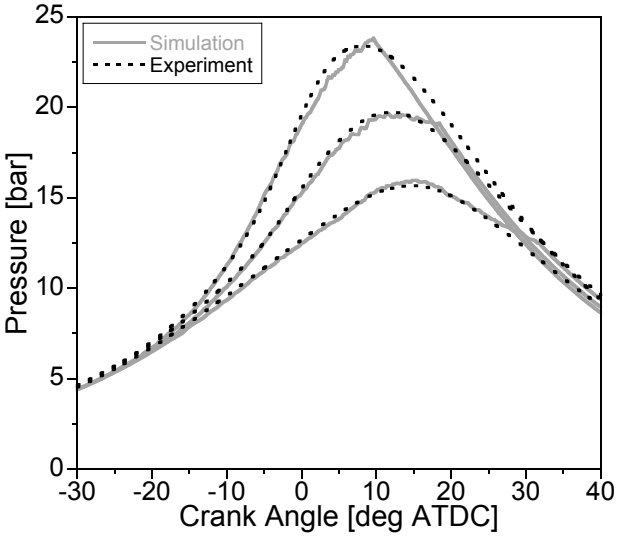

Figure 2: *Fast medium and slow cycles obtained by varying C compared with experiment.*

The physical population of soot aggregates is represented numerically by an ensemble of stochastic soot particles, and, just as with the SRM, any physical prediction must be asymptotically independent of the number of stochastic particles.

3 Model Calibration

The SRM was used to simulate a four-cylinder, in-line, four-stroke Gasoline Direct Injection (GDI) SI engine. The engine specifications are given in Table 1.

Table 1: *Engine specifications.*

Cylinders	4
Fuel	95 RON gasoline
Bore [mm]	87.5
Stroke [mm]	83.0
Disp. volume [cm^3/cyl]	499
Compression Ratio	12

The engine displayed high cycle-to-cycle variations (CCV) at the speed, 1500 RPM, and load, 2.2 bar IMEP, investigated. Measurements suggested an EGR ratio of 30% at this operating point. Large amounts of internal EGR have been reported to increase CCV [20]. Details of the engine are given in Table 1. A mixture of 95 % iso-octane and 5 % n-heptane were used to simulate the 95 Research Octane Number (RON) gasoline. The model was calibrated to fit an experimental pressure profile from a cycle with a peak pressure close to the average as shown in Figure 2, using 100 stochastic SRM particles.

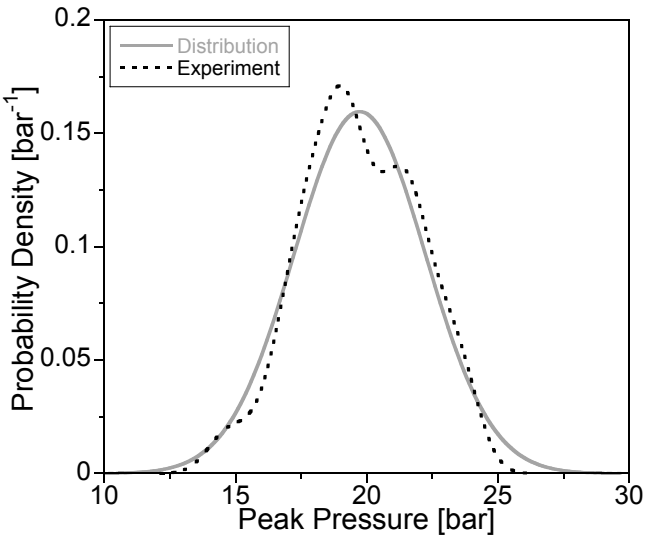

Figure 3: *Normal distribution fit to experimental distribution of peak pressures.*

Figure 2 shows experimental pressure against crank angle and the simulation results when the constant C, from Equation (4), was varied to fit a fast, medium and slow burning cycle. The pressure traces match the experimental data well. The cycles in which the flame initially entrains mass at a faster rate, continue to entrain mass at a fast rate throughout the cycle. This suggests variations in the flame surface area occur early in the cycle resulting in different rates of unburned gas entrainment and combustion. This could be caused by the flame kernel being convected towards a wall, reducing the available area, or due to turbulence altering the shape of the kernel early in the cycle resulting in a higher surface area.

Figure 3 shows the PDF of peak pressure obtained from the experimental data and a normal distribution fitted to the data. The peak pressures measured in the experiment fit a normal distribution well. Using the values from the C sweep, a relationship between peak pressure, in bar, and C was obtained for the 4-cylinder engine. Figure 4 shows C against peak pressure in the cylinder and the curve with equation (5).

$$C = 0.0015{P_{max}}^3 - 0.0545{P_{max}}^2 + 1.8274P_{max} - 10.49. \tag{5}$$

The engine model was coupled with GT-Power, a one dimensional engine simulation tool, to allow multi-cycle simulation. The fitted normal distribution of the experimental peak pressures, with mean 19.7 bar and standard deviation 2 bar, was used to generate a random peak pressure for each simulated cycle. The peak pressure was used to obtain C for the cycle using equation (5). The detailed exhaust gas composition was stored at the end of each cycle and used in the following cycle. The EGR mass was assumed to remain constant. Fifty cycles were simulated and the values of peak pressure against the crank angle they occurred are plotted in Figure 5 along with the experimental results. The simulation matches the experimental data well and the peak pressures do not fall on a straight line but a range of peak pressures were obtained at the same crank angle. This was because the temperature, pressure and composition at IVC are all affected by the

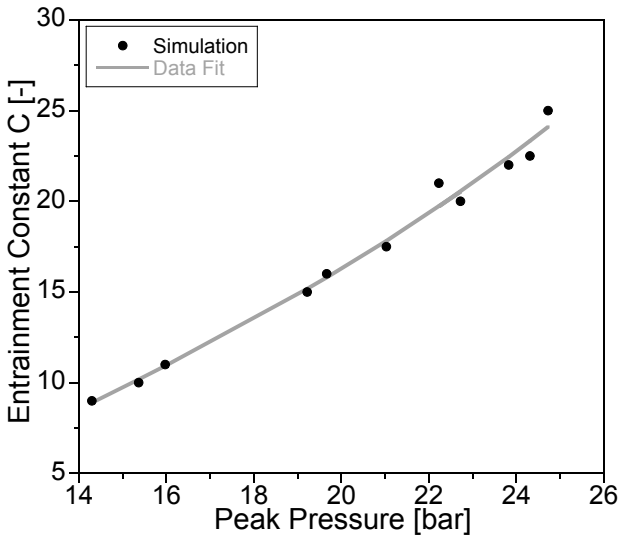

Figure 4: *C against simulated peak pressure.*

Table 2: *Engine specifications.*

Cylinders	4
Fuel	60 % paraffin, 40 % aromatic
Bore [mm]	81.0
Stroke [mm]	89.0
Disp. volume [cm^3/cyl]	457.5
Compression Ratio	12

previous cycle and go ont to affect the current cycle. This is a good result due to the detail required along with short computation times to make a multi-cycle simulation feasible.

4 Results

In this section the model is used to simulate combustion in a DISI engine with late injection causing a stratified charge. Particle size distributions and emissions from the exhaust gas of a 4-cylinder DISI engine at various injection and spark timings have been reported in [30, 31] with the same engine as in [32]. The engine was operated at 1500 RPM with an overall lean fuel air equivalence ratio of 0.58. The engine specifications are given in Table 2. The fuel was modelled as 60 % iso-octane and 40 % toluene. The engine was operated at a range of injection timings and the spark timing in each case set close to MBT. Table 3 gives details of the injection and spark timing in each case.

Simulations were run with identical input parameters, apart from injection and spark timing which were as given in Table 3. A time step of 0.2 CAD was used and 700 stochastic SRM particles. Figure 6 shows how the injection timing effected the stratification in the

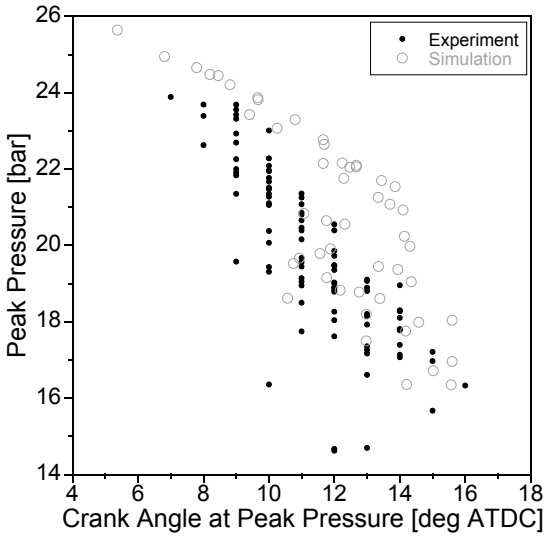

Figure 5: *Peak pressures against crank angle they occurred in 50 simulated and 96 experimental cycles.*

Table 3: *Engine operating conditions.*

Case	1	2	3	4	5
EOI [CAD ATDC]	-50	-60	-70	-75	-80
Spark Timing [CAD ATDC]	-19	-19	-19	-23	-31

simulations. The distribution of equivalence ratios is shown to be greater for the retarded injection timing, as would be expected.

Figure 7 compares the emissions from the engine when the EOI timing was varied in the experiments and simulations. It was found in both experiment and simulation that retarding the injection caused an increase in CO and particle number and a decrease in NO_x emissions. This was due to an increase in the stratification of the cylinder charge as the injection timing was retarded. The higher stratification resulted in richer regions in the cylinder during combustion producing more CO and particles from incomplete combustion. The decrease in NO_x is believed to be due to the lower combustion temperatures reached in the rich and lean combustion that occurs due to stratification. The experimental UHC emissions increased as the injection was retarded. This was the opposite to the trend produced by the simulation. The model does not account for wall impingement, which is likely to cause UHC emissions in the experiment.

Figure 8a shows that retarding the injection timing caused an increase in number density and size of particles in the exhaust gas. Retarding the injection timing in the simulation also caused an increase in the size of particles and total number of particles as shown in Figure 8b. The injection timing had less of an effect on the number of smaller particles in the simulation compared with the experiment.

The change in particle size distribution with time is shown in Figure 9. A decrease in the

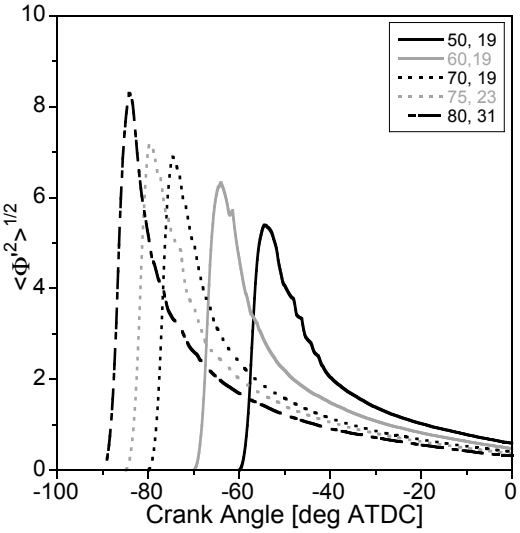

Figure 6: *The root mean square variation in equivalence ratio against crank angle for the different injection timing cases.*

number of particles is seen after combustion as the richer regions are mixed in the overall lean cylinder charge and particles are oxidised as would be expected.

Figure 10 shows the distribution of temperature and pressures in a plot at several crank angles throughout the cycle in the latest EOI case, case 1. In Figure 10a the distribution at the end of injection is shown. The high stratification in equivalence ratio caused by the injection can be seen with equivalence ratios ranging between 0-7.2. The particles with a higher equivalence ratio are at a lower temperature due to fuel evaporation. In Figure 10b, at the spark timing, it can be seen the overall temperature has increased due to compression and the range of equivalence ratio has decreased due to mixing. The stratification continues to decrease and Figure 10 shows the cylinder charge at TDC, at which time a fraction of the particles have burned. The flame propagation continues and in Figures 10c-f an increase in the number of high temperature particles is seen. The particles with equivalence ratios closer to stoichiometric reach a higher temperature as expected.

5 Conclusions

A PDF based Stochastic Reactor Model has been developed to simulate combustion and particulate formation in a Direct Injection Spark Ignition engine. The model incorporates volume change, mixing, heat transfer, direct injection and flame propagation. A detailed chemical mechanism was used along with an in depth soot formation model.

The model was calibrated by simulating a 4-cylinder GDI engine with high cycle to cycle fluctuations in peak pressure. A multi-cycle simulation was done and the peak pressures and crank angle they occurred matched the experimental data well.

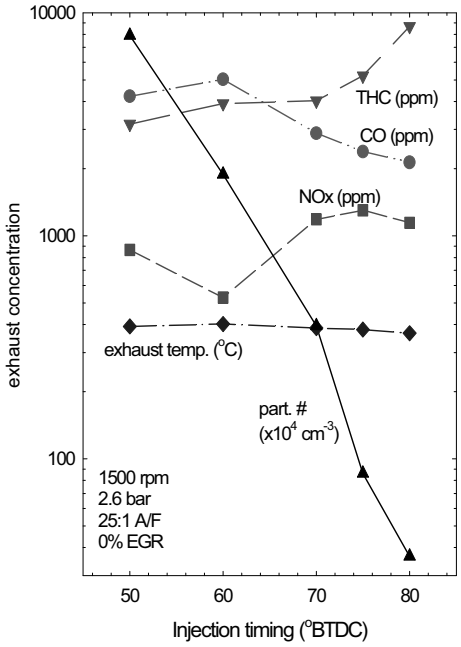

(a) Experiment [30] (reproduced with permission)

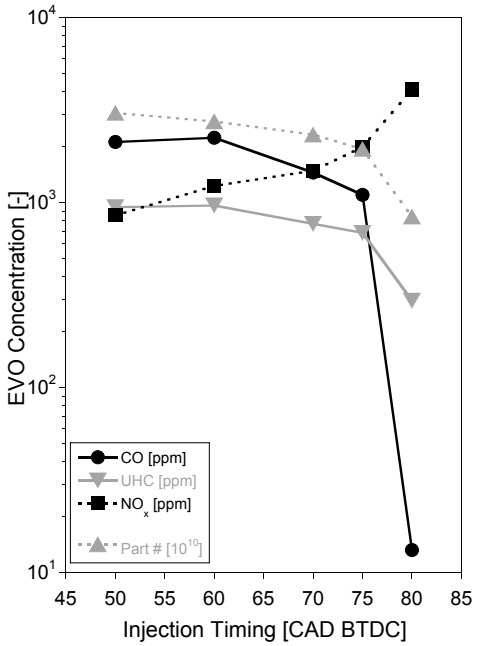

(b) Simulation

Figure 7: *Experimental and simulated emissions for different injection timings.*

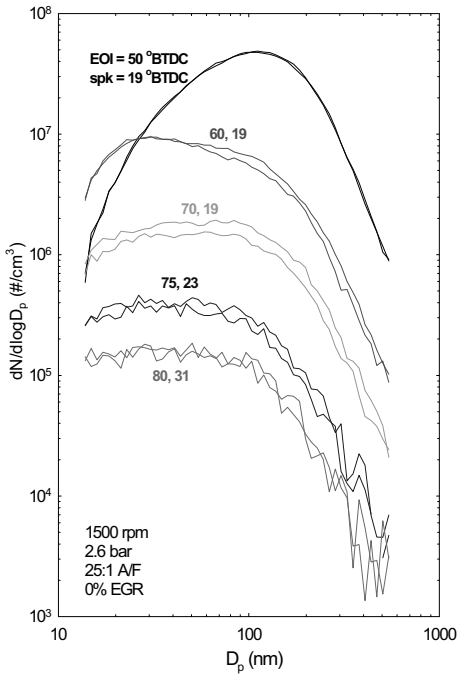

(a) Experiment [30] (reproduced with permission)

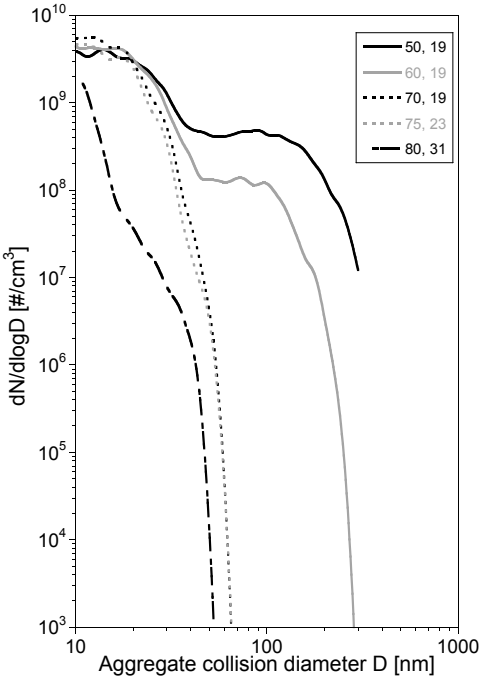

(b) Simulation

Figure 8: *Experimental and simulated particle size distributions for different injection timings.*

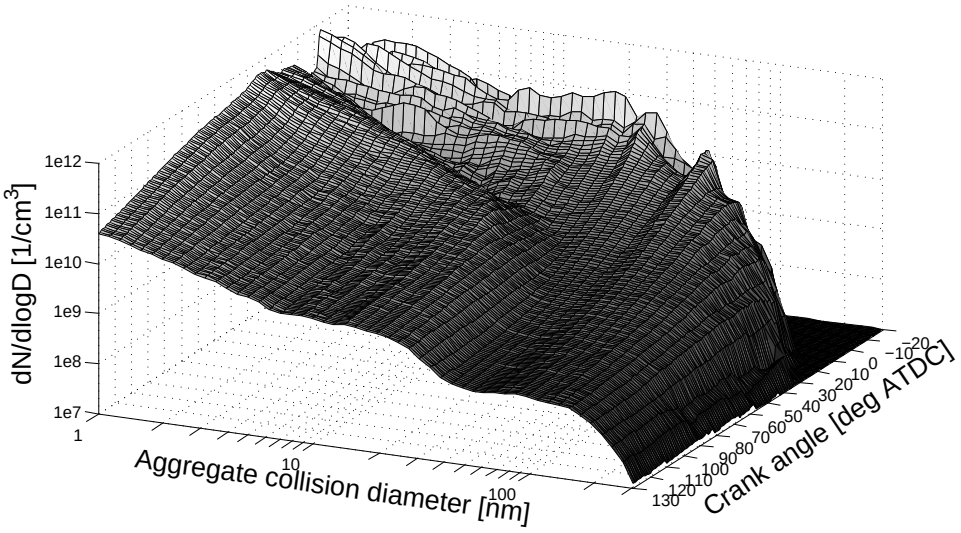

Figure 9: *Time evolution of the size distribution for the EOI -50 CAD ATDC case.*

A 4-cylinder GDI engine operated at low load with high fuel stratification was simulated. The injection timing was varied and a comparison between simulated and experimental emissions made. The model predicted trends in CO, NO_x and particle concentrations well, along with trends in the particle size distribution. An increase in CO and particle emissions was found to occur with a retard in injection timing in both the experiment and simulation. This was due to increased stratification of the fuel causing incomplete combustion in fuel rich regions. The NO_x emissions followed the opposite trend due to the decrease in combustion temperature as the equivalence ratio moves away from stoichiometric.

Acknowledgements

Funding from the EPSRC (UK), grant EP/D068703/1, is gratefully acknowledged. SM would like to thank Churchill College, Cambridge for a Raymond and Beverly Sackler Research Fellowship.

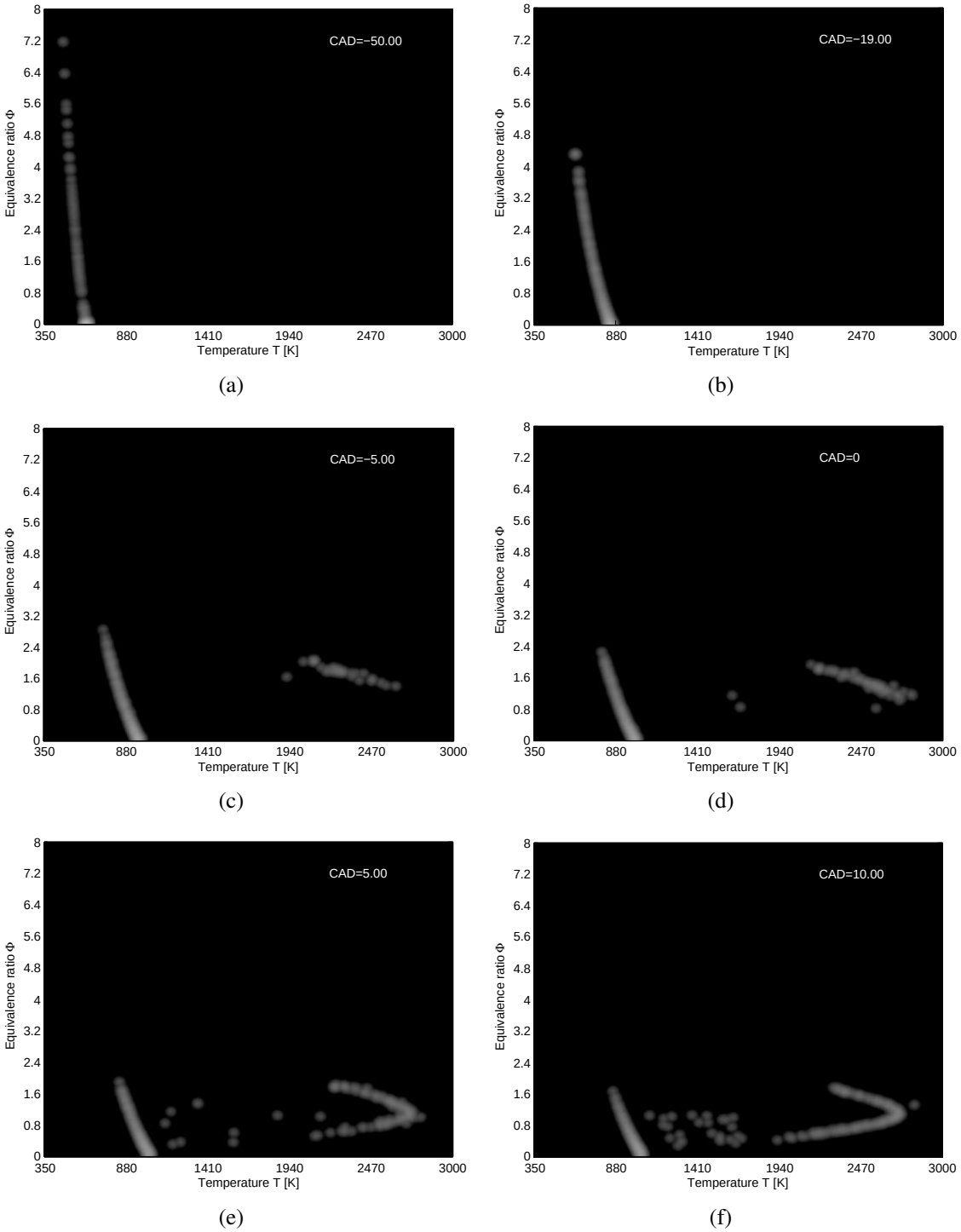

Figure 10: *Time evolution of equivalence ratio and temperature distribution for the EOI -50 CAD ATDC case.*

References

[1] F. Zhao, M.C. Lai, and D.L. Harrington. Automotive spark-ignited direct-injection gasoline engines. *Progress in Energy and Combustion Science*, 25:437–562, 1999.

[2] P. Eastwood. *Particulate Emissions from Vehicles*. Wiley-PEPublishing Series, John Wiley & Sons, 2008.

[3] B.A. Baritaud, J.M. Duclos, and Fusco A. Modeling turbulent combustion and pollutant formation in stratified charge SI engines. *Symposium (International) on Combustion*, 26(2):2627–2635, 1996.

[4] S. Cant and J. Ranasinghe. A Turbulent Combustion Model for a Stratified Charged, Spark Ignited Internal Combustion Engine. SAE Paper No. 2000-01-0275, 2000.

[5] M.C. Drake, T.D. Fansler, and A.M. Lippert. Stratified-charge combustion: modeling and imaging of a spray-guided direct-injection spark-ignited engine. *Proceedings of the Combustion Institute*, 30:2683–2691, 2005.

[6] R. Dahms, T.D. Fansler, M.C. Drake, T.-W. Kuo, A.M. Lippert, and N. Peters. Modeling ignition phenomena in spray-guided spark-ignited engines. *Proceedings of the Combustion Institute*, 32:2743–2750, 2009.

[7] A. Kazakov and D.E. Foster. Modeling of soot formation during DI Diesel combustion using multi-step phenomenological model. SAE Paper No. 982463, 19988.

[8] G.J. Micklow and W. Gong. A multistage combustion model and soot formation model for direct-injection diesel engines. *Proceedings of the Institute of Mechanical Engineers, Part D: Journal of Automobile Engineering*, 216(6):495–504, 2002.

[9] S. Hong, M.S. Woolridge, H.G. Im, D.N. Assanis, and H. Pitsch. Development and application of a comprehensive soot model for 3D CFD reacting flow studies in a Diesel engine. *Combustion and Flame*, 143:11–26, 2005.

[10] J. Bouolanger, F. Liu, W.S. Neill, and G.J. Smallwood. An improved soot formation model for 3D diesel engine simulations. *Journal of Engineering for Gas Turbines and Power*, 129(3):877–884, 2007.

[11] S. Mosbach, M.S. Celnik, A. Raj, M. Kraft, H.R. Zhang, S. Kubo, and K.O. Kim. Towards a detailed soot model for internal combustion engines. *Combustion and Flame*, 156(6):1156–1165, 2009.

[12] S. B. Pope. PDF methods for turbulent reactive flows. *Prog. Energy Combust. Sci.*, 11:119–192, 1985.

[13] S. Subramaniam and S. B. Pope. A Mixing Model for Turbulent Reactive Flows based on Euclidean Minimum Spanning Trees. *Combustion and Flame*, 115:487–514, 1998.

[14] H. Su, A. Vikhansky, S. Mosbach, M. Kraft, A. Bhave, K. Kim, T. Kobayashi, and F. Mauss. A computational study of an HCCI engine with direct injection during gas exchange. *Combustion and Flame*, 147:118–132, 2006.

[15] M. Kraft, P. Maigaard, F. Mauss, M. Christensen, and B. Johansson. Investigation of combustion emissions in a homogeneous charge compression injection engine: Measurements and a new computational model. *Proceedings of the Combustion Institute*, 28:1195–1201, 2000.

[16] A. Bhave, M. Kraft, L. Montorsi, and F. Mauss. Sources of CO emissions in an HCCI engine: A numerical analysis. *Combustion and Flame*, 144:634–637, 2006.

[17] S. Mosbach, A. Aldawood, and M. Kraft. Real-Time Evaluation of a Detailed Chemistry HCCI Engine Model Using a Tabulation Technique. *Combustion Science and Technology*, 180:1263–1277, 2008.

[18] J. Etheridge, S. Mosbach, M. Kraft, H. Wu, and N. Collings. Investigating Cycle to Cycle Variations in an SI Engine Through Experiments and a New Computational Model. Submitted for publication. Also available as Technical Report 62, c4e Preprint Series, Cambridge, 2008.

[19] J. Tagalian and J. Heywood. Flame Initiation in a Spark-Ignition Engine. *Combust. Flame*, 64:243–246, 1986.

[20] J. B. Heywood. *Internal Combustion Engine Fundamentals*. McGraw-Hill, New York, 1988.

[21] H. Daneshyar and P. G. Hill. The structure of small-scale turbulence and its effect on combustion in spark ignition engines. *Prog. Energy Combust. Sci.*, 13:47–73, 1987.

[22] J. Keck. Turbulent flame structure and speed in spark-ignition engines. *Nineteenth Symposium (International) on Combustion/The Combustion Institute*, pages 1451–1466, 1982.

[23] R.L. Curl. Dispersed phase mixing: 1. Theory and effects in simple reactors. *AIChE Journal*, 9(2):175181, 1963.

[24] M. Goodson and M. Kraft. An Efficient Stochastic Algorithm for Simulating Nanoparticle Dynamics. *Journal of Computational Physics*, 183(1):210–232, 2002.

[25] M. Balthasar and M. Kraft. A stochastic approach to calculate the particle size distribution function of soot particles in laminar premixed flames. *Combustion and Flame*, 133(3):289–298, 2003.

[26] M.S. Celnik, R.I.A. Patterson, M. Kraft, and W. Wagner. Coupling a stochastic soot population balance to gas-phase chemistry using operator splitting. *Combustion and Flame*, 148(3):158–176, 2007.

[27] M.S. Celnik, A. Raj, R.H. West, R.I.A. Patterson, and M. Kraft. Aromatic site description of soot particles. *Combustion and Flame*, 155(1–2):161–180, 2008.

[28] A. Raj, M.S. Celnik, R.A. Shirley, M. Sander, R.I.A. Patterson, R.H. West, and M. Kraft. A statistical approach to develop a detailed soot growth model using pah characteristics. *Combustion and Flame*, 156:896–913, 2009.

[29] R.I.A. Patterson, J. Singh, M. Balthasar, M. Kraft, and J.R. Norris. The Linear Process Deferment Algorithm: A new technique for solving population balance equations. *SIAM Journal on Scientific Computing*, 28(1):303–320, 2006.

[30] M.M. Maricq, D.H. Podsiadlik, D.D. Brehob, and M. Haghgooie. Particulate Emissions from a Direct-Injection Spark-Ignition DISI Engine. SAE Paper No. 1999-01-1530, 1999.

[31] E.W. Kaiser, W.O. Siegl, D.D. Brehob, and M. Haghgooie. Engine-Out Emissions from a Direct-Injection Spark-Ignition DISI Engine. SAE Paper No. 1999-01-1529, 1999.

[32] D.D. Brehob, J.E. Fleming, M. Haghgooie, and R.A. Stein. Stratified-Charge Engine Fuel Economy and Emission Characteristics. SAE Paper No. 982704, 1998.